

Post-seismic infrastructure damage assessment using high-resolution SAR satellite data

Timo Balz^{*a}, Daniele Perissin^b, Uwe Soergel^c, Lu Zhang^a, Mingsheng Liao^a

^aState Key Laboratory of Information Engineering in Surveying, Mapping and Remote Sensing, Wuhan University, P.R. China;

^bPolitecnico di Milano, Italy;

^cInstitute of Photogrammetry and GeoInformation, Leibniz University Hannover, Germany

ABSTRACT

The Wenchuan Earthquake on May 12, 2008, devastated a vast area in Sichuan, China. The swift rescue and disaster management measures of the Chinese government have been supported by radar remote sensing from the very beginning. The new high-resolution synthetic aperture radar (SAR) satellites, like COSMO-SkyMed and TerraSAR-X, have been used for damage assessment and rapid mapping. Unfortunately, only one stripmap image from the area was acquired by COSMO-SkyMed before the earthquake, allowing therefore the generation of only one co-seismic interferogram over a limited area to evaluate the motion of the terrain. Thorough analysis of the acquired data can reveal the status of buildings and infrastructure using only post-seismic high-resolution images. In this paper, damaged bridges and dams will be analyzed and strategies for damage detection in SAR images will be discussed. Typical signatures of damaged bridges will be shown and long-time monitoring of dams using SAR is demonstrated.

Keywords: Radar, SAR, Earthquake, Bridge, Damage Assessment, High-Resolution, PSI

1. INTRODUCTION

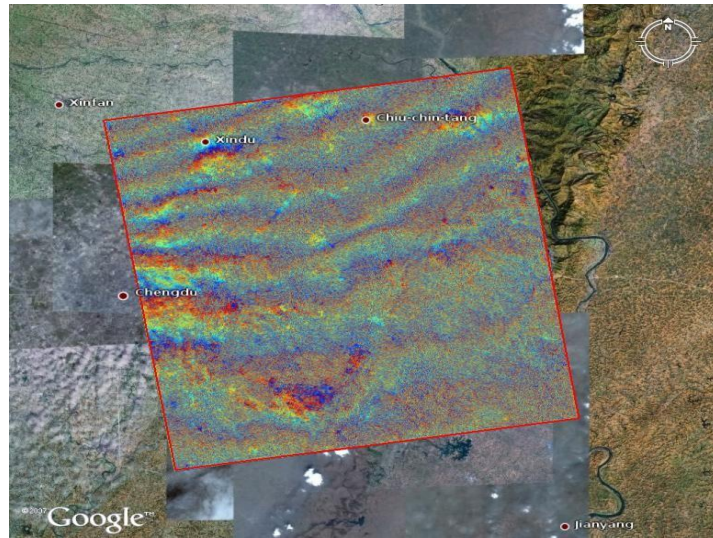
On May 12, 2008, the Wenchuan Earthquake with a magnitude of 7.9 devastated a huge area in the Sichuan Province of China. The epicenter was in Wenchuan, northwest of Chengdu, the capital of the Sichuan province [1]. The rupture propagated for about 270km north-northeast alongside the “Dragon’s Gate Mountains (Long Men Shan)” [2]. High-resolution synthetic aperture radar (SAR) satellite images supported the rescue and disaster management operations in the area. The independence of radar from weather and daylight proved to be particularly useful in disaster management and rescue operations, because heavy rainfall and cloud coverage hindered the use of optical remote sensing systems in the days following the earthquake.

SAR, especially interferometric SAR, is widely used for the analysis of earthquakes and earthquake related damages [3]. A range of works has been published about post-seismic building damage assessment, using pre- and post-earthquake data [4-5]. Although bridges are of utmost importance for post-disaster logistics, there is not much research work published about the detection of damaged bridges in SAR images [6]. One reason might be that the spatial resolution of mid-resolution SAR systems, like ERS, JERS, Radarsat-1, etc., is not sufficient for detecting bridge damages [7].

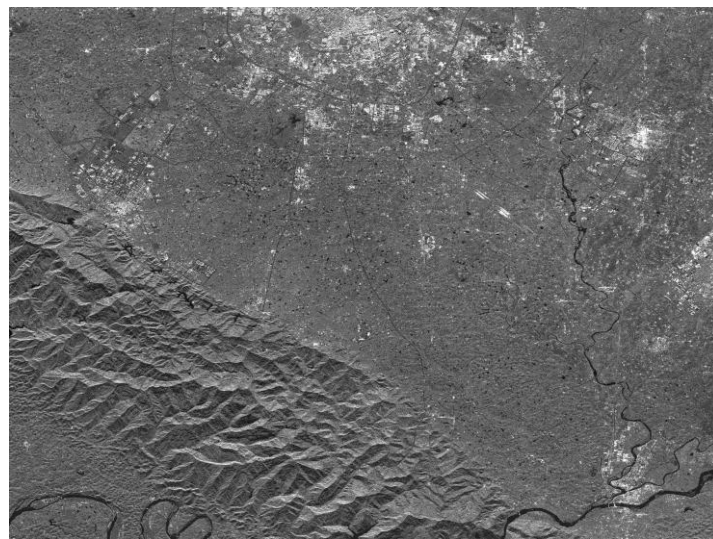
High-resolution SAR data could deliver even more precise results. Unfortunately, high-resolution change detection could not be applied using TerraSAR-X, because the sensor is just operational since early 2008 and did not acquire any pre-seismic data from the devastated area. COSMO-SkyMed took one image over Chengdu in stripmap mode on April 13. A second image along the same orbit was planned soon after the seism and taken on May 15 (three days after the shake). The co-seismic interferogram generated from the two acquisitions is shown in Fig. 1. The imaged area has an extension of 40x40 km² and the spatial resolution is about 3x3 m². The normal baseline is 71m and the temporal one 32 days. Fig. 1(a) shows the geo-referenced differential interferogram (after compensating for the topography provided by SRTM data) and Fig 1(b) reports its amplitude in SAR coordinates. The interferometric fringes show with impressive details the

* balz@lmars.whu.edu.cn; phone +86 15071459772; www.lmars.whu.edu.cn

ground shift occurred during the seism. The obtained coherence is remarkable even in vegetated parts of the analyzed area (low right in (a), low left in (b)) highlighting the great potential of high-resolution data for monitoring ground motions.



(a)



(b)

Fig. 1. (a) COSMO-SkyMed co-seismic interferogram over Chengdu superimposed to a Google-Earth optical image; (b) amplitude of the interferogram in SAR coordinates. The work was carried out within a collaboration between Politecnico di Milano (POLIMI) and the Department of Civil Protection of Italy. The data were processed by the POLIMI spin-off companies TRE and Aresys.

Directly after the earthquake, the focus of the authorities and the spatial data service providers was the fast coverage of the area with newly acquired post-earthquake data. To cover a huge area fast, stripmap data was acquired for most of the area. Only few areas of interest have been acquired in spotlight mode. For the post-earthquake analysis, single polarized stripmap data with around three meter resolution had to be used.

The status of the infrastructure, especially roads and bridges, is of utmost importance for the rescue operations in the aftermath of an earthquake. Bridges are vulnerable key points of the infrastructure and the damage assessment of bridges

is one of the most urgent needed intelligence information for post-disaster logistics. Dams are endangered by earthquakes and the collapse of a dam could cost the lives of thousands of people.

In the following section, some theoretical background about the appearance of bridges in SAR images will be presented. In section 3, the damage assessment of bridges and dams will be exemplarily demonstrated using examples from Sichuan. Multi-image analysis for dam monitoring is presented in section 4. Finally conclusions are drawn.

2. APPEARANCE OF BRIDGES IN HIGH-RESOLUTION SAR IMAGES

2.1 High-resolution SAR image geometry

SAR systems are side-looking radar systems. The oblique viewing geometry is crucial for SAR processing as well as for understanding SAR image geometry. The geometry of SAR images differs in azimuth and range direction. SAR needs a moving platform to make use of the Doppler Effect, improving the resolution in azimuth direction. The position of an object in azimuth direction is determined by the Doppler Shift. Therefore the position of moving objects can be disturbed, but fixed objects, like buildings and bridges, will be positioned correctly and precisely in azimuth direction.

The SAR geometry in range direction depends on the running time of the signal between the sensor, the backscattering object, and the receiving antenna. Ignoring atmospheric effects, the running time of the signal directly corresponds to the travelling distance of the signal. The distance between the elevated parts of objects, e.g. building roofs, and the sensor is smaller than that between the lower part and the sensor, therefore the elevated parts are mapped closer to the sensor. This effect is called layover and is typical for SAR images in urban areas.

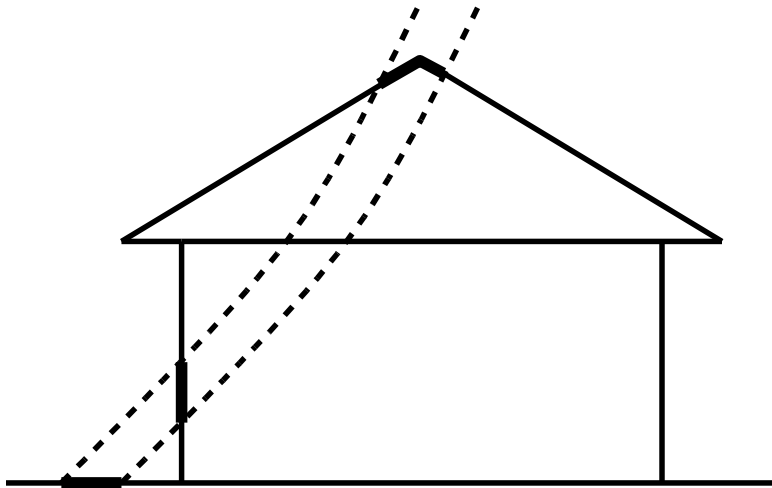


Fig. 2. Ambiguous building backscatter.

Different parts of an elevated object are, depending on the spatial resolution of the system, mapped at the same position. As exemplarily shown in Fig. 2, parts of the roof, the building wall and the area in front of the building have the same distance to the sensor. The backscatter of these parts is received simultaneously by the receiving antenna and the backscatter of these different parts will be mixed up.

Another important geometrical effect is caused by double- and multi-bounce reflections. Double-bounces can occur when a radar signal is scattered by a building wall to the ground and from the ground back to the radar sensor. Triple-bouncing can occur when a radar signal is scattered from a building wall to a backscattering surface, subsequently back to the wall, and from the wall back to the receiving antenna. Regarding buildings surrounded by streets, which typically can be described as 90° dihedrals with flat surfaces in relation to the wavelength, it is shown that multi-bounces do not arise [8]. Triple bouncing frequently occurs in SAR images of bridges of water [9-10], which will be shown in section 2.2.

An interesting fact of double-bouncing of 90° dihedrals with flat surfaces is the fact that all double-bounces occurring between the dihedral have the same length. They are therefore all received by the sensor antenna at the same time.

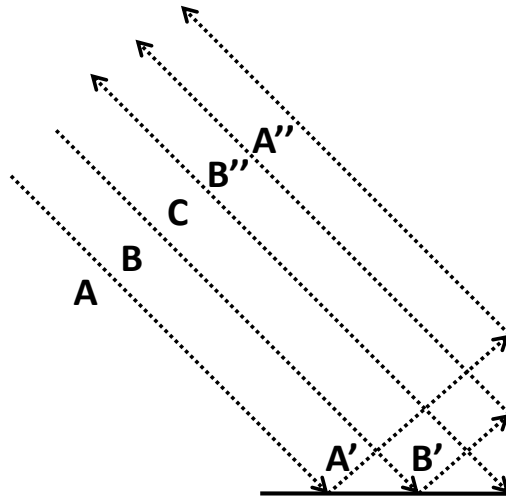


Fig. 3. Double-bouncing of a 90° dihedral.

The situation is sketched in Fig. 3. The distance of each double-bounce is the same as two times the distance between the foot point of the dihedral and the sensor:

$$2 \cdot \bar{C} = \bar{A} + \bar{A}' + \bar{A}'' = \bar{B} + \bar{B}' + \bar{B}''$$

This leads to a very strong overall reflection occurring at the location of the foot point, due to the incoherent summation of the various double-bounce reflections

2.2 Appearance of bridges in high-resolution SAR images

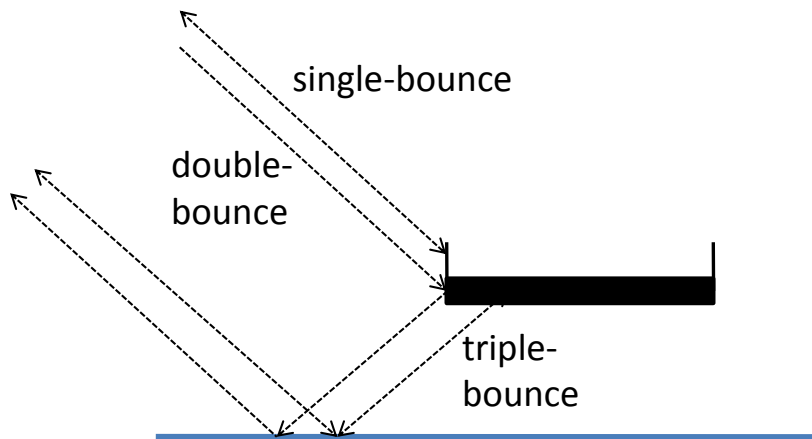


Fig. 4. Backscatter of a bridge over calm water.

Bridges over water are typically clearly recognizable in SAR images, because the strong reflection from bridges highly contrasts with the dark appearance of water in SAR images. Calm water acts like a mirror to the oblique SAR signal; hence, almost no backscatter returns to the sensor. Bridges over calm water typically have three clearly visible reflections from near-range to far-range direction:

1. the single-bounce reflection, caused by a direct reflection of the bridge;
2. the double-bounce reflection, caused by reflections from the bridge to the water and back to the sensor (or vice versa);
3. the triple-bounce reflection, caused by reflections from the water to the bridge back to the water and finally back to the sensor.

This is exemplarily illustrated in Fig.4. In SAR scenes with an aspect angle $\phi \approx 90^\circ$ between the orientation of the bridge and the azimuth direction of the SAR platform, or in scenes with bridges over turbulent water, these features are not visible.

Often superstructures of bridges are also visible [11], like for example in Fig.5 depicting a SAR image of a bridge over relatively calm water in Wuhan. The scene in Fig.5 is not geo-referenced. The sensor is illuminating the scene from the left side. On the left side, near-range of the bridge, the single-bounce reflection of the bridge and the superstructures are visible, followed by the brighter double-bouncing. The triple-bouncing far-range of the bridge is weaker and blurred due to small perturbations of the water.

By measuring the distance between the double-bounce reflection of the bridge R_{db} in ground-range and the ground-range single-bounce reflection R_{sb} the height of the bridge above water h can be determined with the incidence angle θ_i [12].

$$h = (R_{db} - R_{sb}) / \cos(\theta_i)$$

Instead of the single-bounce, the triple-bounce position R_{tb} can also be used:

$$h = (R_{tb} - R_{db}) / \cos(\theta_i)$$

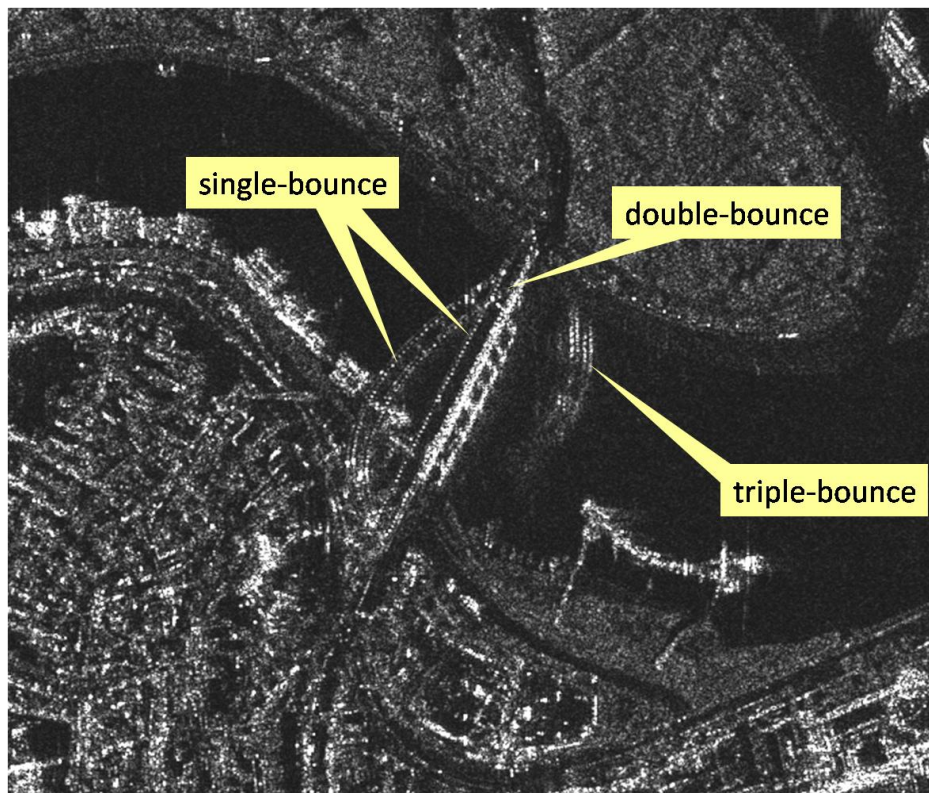
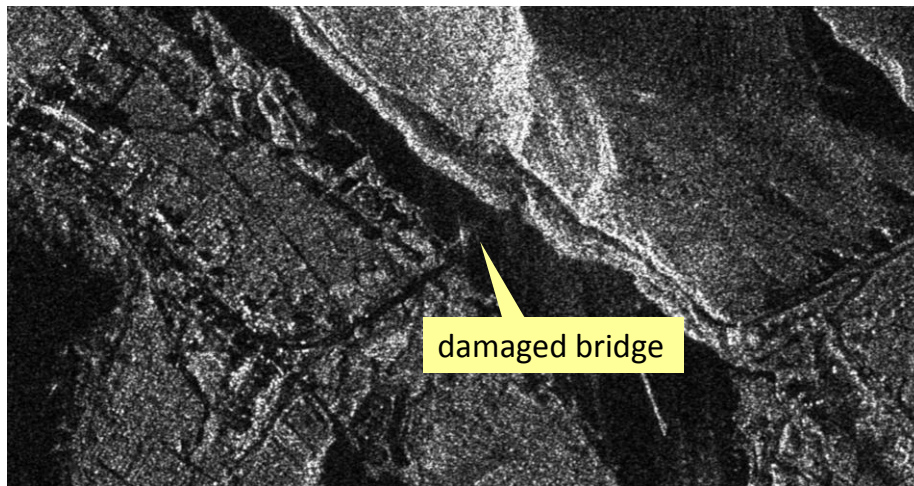


Fig. 5. TerraSAR-X spotlight image showing a road bridge connecting Hanyang and Hankou in Wuhan, China.

3. DAMAGE ASSESSMENT IN POST-EARTHQUAKE SAR IMAGES

3.1 Analyzing bridges in post-earthquake SAR images



(a)



(b)

Fig. 6. TerraSAR-X spotlight images showing a bridge south of Maowen (a) and a bridge in the center of Maowen (b). Image acquired on May 16, 2008, from an ascending orbit.

In Fig. 6 two geo-referenced TerraSAR-X spotlight images of damaged bridges in Maowen and south of Maowen are depicted. The images were acquired from an ascending orbit; hence, the sensor was heading around 350° and illuminated the scene from the left side. The remaining parts of the bridges are clearly visible. The damage of the bridges can be identified by the missing parts of the bridges. The bridge in Fig. 6(a) ends in the middle of the water and in (b) a part of the bridge is missing. The images are taken from an ascending orbit; therefore, the mountains east of the bridge in Fig. 6(a) do not cast any shadow on the bridge. This is important, because shadows casted on bridges can be mistaken as bridge damage.

In Fig.7 a bridge near Duanjiangyan city can be seen. The typical single-, double-, triple bounce combination is clearly visible, especially in the images of May 15 and May 22. The bridge appears to be undamaged. But besides analyzing damages, bridges in SAR images can also provide useful information about the water level. On May 13, 2008, the water is around 8m above the water level. The water level dropped afterwards. On May 15, the bridge was approximately 9.2m

above the water level, whereas on May 22 the bridge was around 10.4m above the water level. The level rose back and on June 6 the bridge is approximately 8.5m above the water level. Using the equations from section 2.3 this can conveniently be calculated using the incidence angle, which is 49° in the COSMO-SkyMed image from May 13, 46.85° at the scene center in the image taken on May 15 and 35.09° in the image acquired on May 22. The different water levels can also be recognized downstream of the bridge.

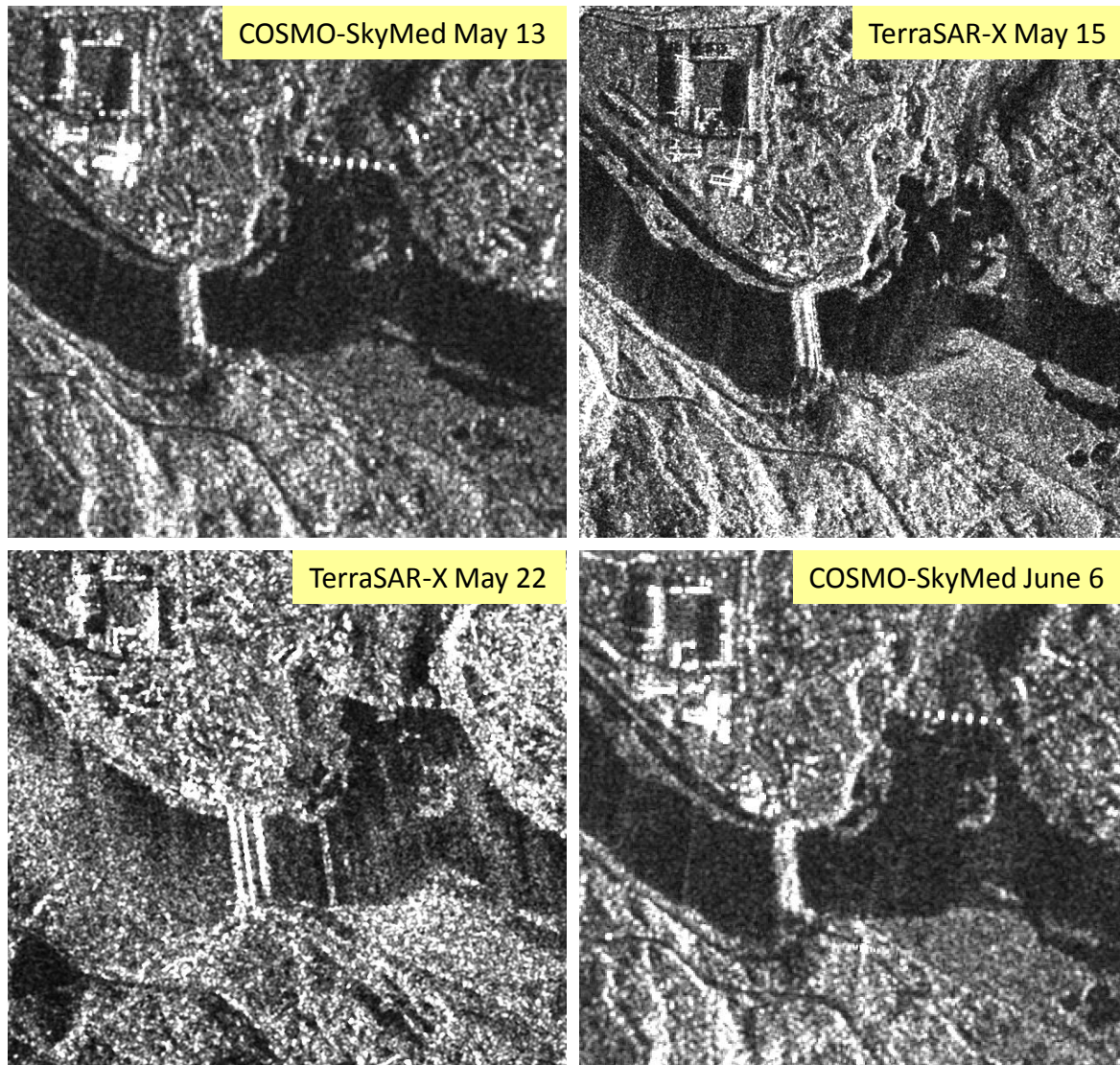


Fig. 7. Subsets of two COSMO-SkyMed and two TerraSAR-X images showing a bridge northwest of Duanjiangyan city.

Fig.8 shows the bridge south of Anchang town. The bridge seems to be undestroyed in the image on the left side, but appears to be destroyed in the image on the right side. The different appearances are caused by the different water levels. In the image taken on May 15, the water level is high and the bridge shows a clear structure in the SAR image. Due to the lower water level on May 17, there is no clear double-bouncing between the bridge and the water and the dry river ground is backscattering in the vicinity of the bridge. This example demonstrates the difficulty of SAR data interpretation. Attention has to be paid not only to the sensor properties, but also to the changes in the environment while examining multi-temporal datasets.

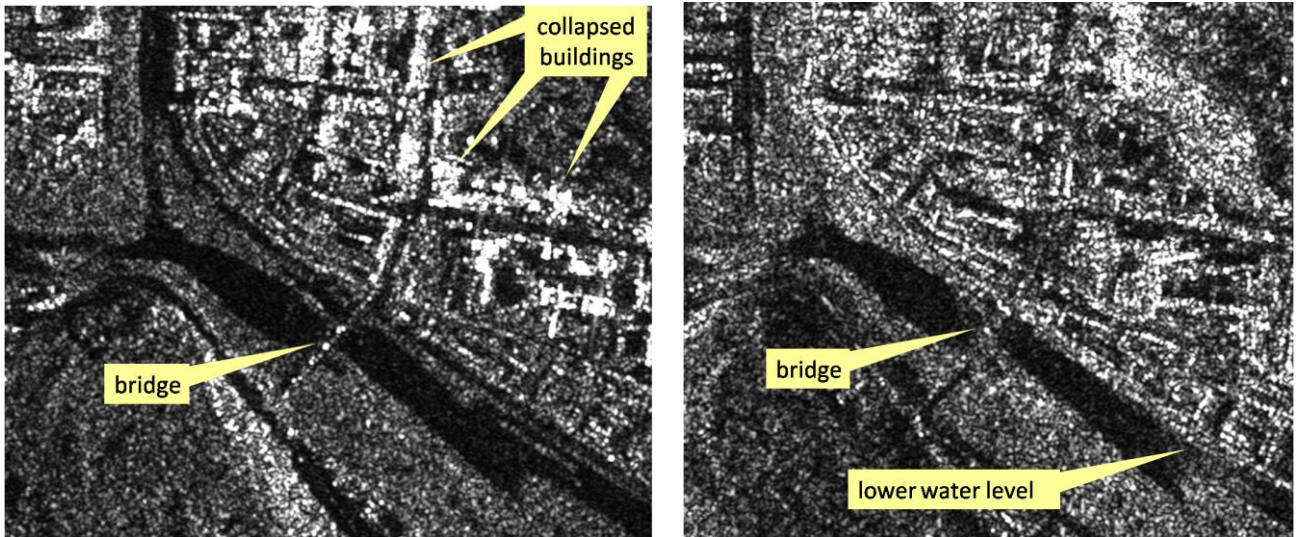
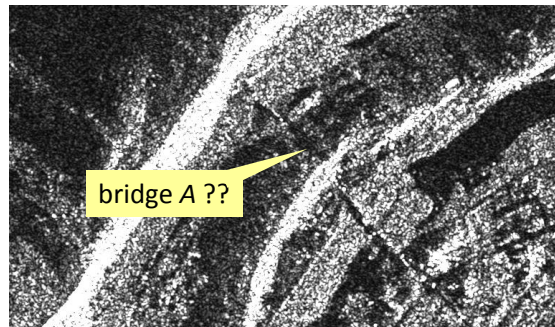
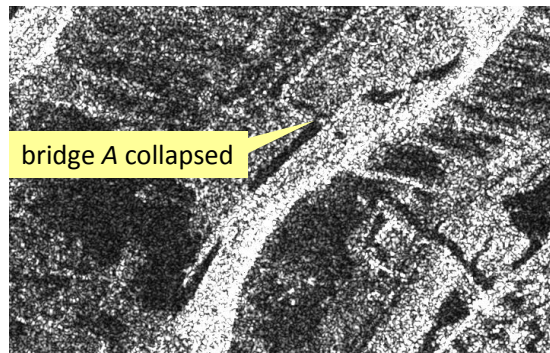


Fig. 8. Two TerraSAR-X stripmap images showing a bridge south of Anchang Town. Left side acquired on May 15, 2008 from a descending orbit; right side acquired on May 17, 2008 from an ascending orbit.

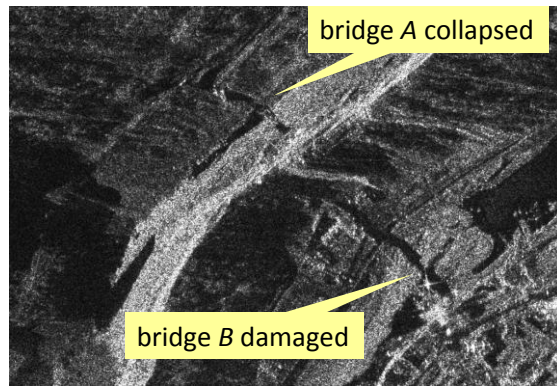
In Fig. 9, three SAR images showing two bridges in the center of the Beichuan county town can be seen. Bridge A collapsed due to the earthquake and bridge B was heavily damaged. In Fig. 9(a) the status of bridge A cannot be determined. Beichuan resides in a deep valley and is surrounded by steep mountain ridges. In the image acquired from a descending orbit, the valley of bridge A is fore-shortened to just a few pixels. The bridge is barely recognizable and the status of the bridge is unidentifiable. Bridge B seems undamaged in both stripmap images at Fig. 9(a) and (b). It requires the higher resolution of a spotlight image to identify the damage. In Fig. 9(c) the partial destruction of bridge B is clearly identifiable due to the shadow casted by the bridge. The collapse of bridge A is also identifiable in the spotlight image.



(a)



(b)



(c)

Fig. 9. Three SAR images showing the status of two bridges in Beichuan county town. (a) TerraSAR-X stripmap image acquired from a descending orbit on May 15, 2008; (b) TeraSAR-X stripmap image acquired from an ascending orbit on May 22, 2008; (c) COSMO-SkyMed spotlight image acquired from an ascending orbit on May 14, 2008.

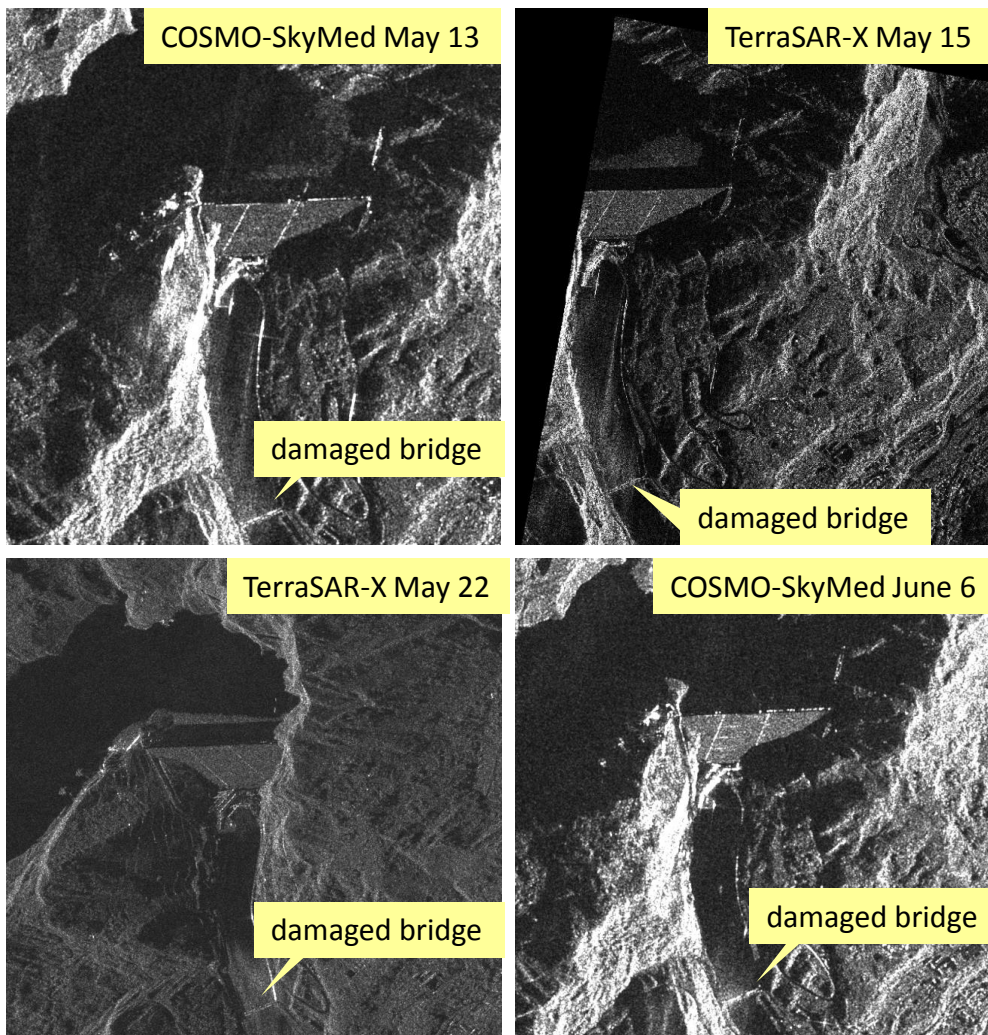


Fig. 10. Subsets of two COSMO-SkyMed and two TerraSAR-X images showing the Zipingpu Dam.

In Fig.10 a series of high-resolution SAR images showing the Zipingpu Dam can be seen. The Zipingpu Dam, just 500 meters from the fault that failed and 5.5 kilometers from the quake's epicenter [13], was a high-priority object for post-earthquake surveillance. Due to its close proximity to the fault line, there were raising concerns about the stability of the dam. The first post-earthquake COSMO-SkyMed image from May 13 acquired data of the dam and the first TerraSAR-X spotlight image of the disaster area, taken on May 15, also surveyed the situation of the dam and of Duanjiangyan city below the dam. Fortunately, the concerns were unfounded as the dam suffered only minor damages [14]. The bridge to the south of the dam collapsed though, as can be seen in Fig.10.

4. MULTI IMAGE ANALYSIS FOR DAM MONITORING

Whenever repeated images over the same area are available, more advanced analysis become possible. As shown in [15], exploiting many repeated spaceborne SAR acquisitions at a relatively low resolution (~25m x 5m on the ground), the 3D position of stable targets can be estimated with sub-meter accuracy. Moreover, by analyzing scattering pattern and polarimetric response of the targets, their main radar characteristics can be estimated and a system for automatic detection of manmade target typologies (resonating structures, mirrors, poles, dihedrals and trihedrals) can be developed. The interpretation of millimetric deformations detected by the radar can then be improved and the identification of multi-sensor targets allows the combination of data acquired with different orbits, frequencies and polarizations, increasing the number of deformation measurements and the number of detected targets [16].

Unfortunately over the earthquake area of interest no data stack is available at this moment. More in general, high-resolution spaceborne archives are still being acquired. To give an idea of what could be achieved with time series of high resolution SAR data, we briefly report the results got by analyzing 40 Envisat images over the Three Gorges Dam, spanning the period 2003-2008. Fig.11 shows all the detected Permanent Scatterers on the dam [17-18], indicating with a color scale their height with respect to a reference point in the image. Fig.12 reports the millimetric deformation time series estimated for two Permanent Scatterers on the dam. As visible from Fig.12, a slight seasonal trend can be appreciated, likely due to the seasonal character of the Yangtze river, generating a higher pressure on the dam when the water level increases.

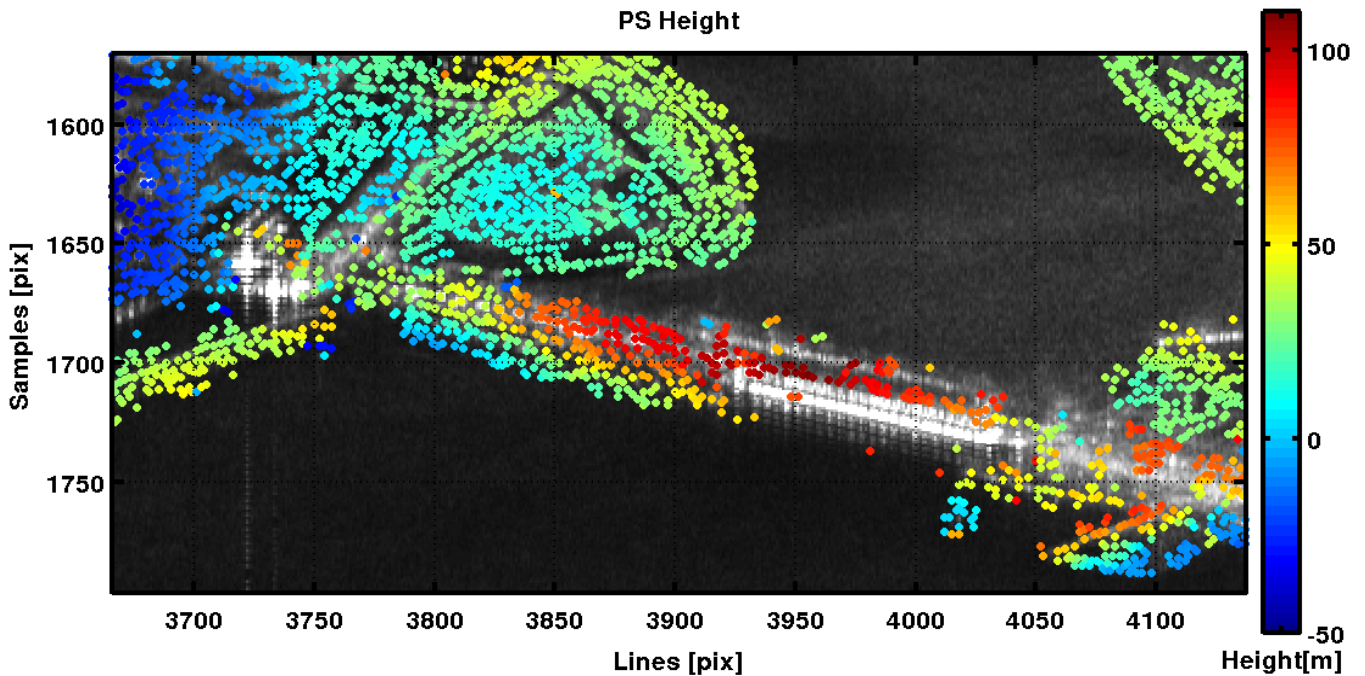


Fig. 11. Permanent Scatterers detected on the Three Gorges Dam. Color scale: estimated height w.r.t a reference point.

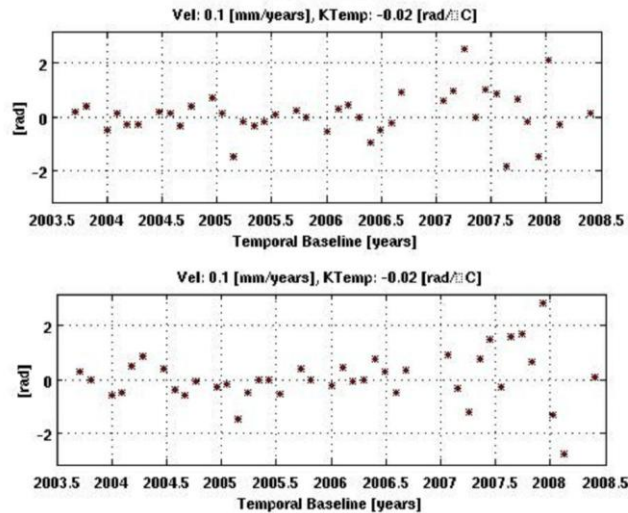


Fig. 12. Deformation time series examples for two Permanent Scatterers detected on the Three Gorges Dam.

5. CONCLUSION

Using high-resolution spaceborne SAR systems, damaged and collapsed bridges can be identified, but the identification of damaged bridges using only one single SAR image is difficult. Using high-resolution spotlight data increases the ability to assess bridge damages correctly. High resolutions are crucial and using very high-resolution SAR systems is most beneficial for the detection of damaged buildings [19-20] and bridges, but such airborne systems are not available in many countries. In disaster management though, even the spotlight mode of high-resolution SAR satellite systems can seldom be used if a large area is affected by the disaster and has to be covered as fast as possible.

Persistent Scatterer Interferometry (PSI) is an important tool in risk analysis. Besides monitoring dams and bridges, PSI can also be used for subsidence monitoring. The subsidence information gained from PSI can be used for mapping areas endangered by landslides. Knowing which areas are endangered by earthquake induced landslides, can support the post-disaster image interpretation.

SAR proved to be particularly useful for disaster management in the aftermath of the Wenchuan Earthquake. Damaged infrastructure was recognized in high-resolution SAR images independently from the weather, at day and night. Furthermore, the co-seismic interferogram, shown in Fig. 1, proves the great potential of the new generation of high-resolution SAR satellites for ground motion monitoring.

ACKNOWLEDGMENT

The authors would like to thank the Infoterra GmbH, Beijing Spot Image, and Beijing Earth Observation Inc. for their help and support. Parts of the work in the paper were supported by the National Key Basic Research and Development Program of China (Contract No. 2007CB714405) and China Postdoctoral Science Foundation (20080440952).

REFERENCES

- [1] Stone, R., "An Unpredictably Violent Fault", *Science* 320, 1578-1580 (2008).
- [2] Royden, L.H., Burchfiel, B.C. and van der Hilst, R.D., "The Geological Evolution of the Tibetan Plateau," *Science* 321, 1054-1058 (2008).
- [3] Massonnet, D., Rossi, M., Carmona, C., Adragna, F., Peltzer, G., Feigl, K. and Rabaute, T., "The displacement field of the Landers earthquake mapped by radar interferometry," *Nature* 364, 138-142 (1993).
- [4] Yonezawa, H.A. and Takeuchi, S., "Decorrelation of SAR data by urban damage caused by the 1995 Hoyoogoken-Nanbu earthquake," *International Journal of Remote Sensing* 22, 1585-1600 (2001).
- [5] Matsuoka, M., Yamazaki, F. and Ohkura, H., "Damage mapping of the 2004 Niigata-ken Chuetsu earth-quake using Radarsat images," *Proc. 2007 Urban Remote Sensing Joint Event, Paris, France* (2007).
- [6] Gamba, P., Dell'Acqua, F. and Trianni, G., "Rapid Damage Detection in the Bam Area Using Multitemporal SAR and Exploiting Ancillary Data," *IEEE Transactions on Geoscience and Remote Sensing* 45, 1582-1589 (2007).
- [7] Adams, B., Huyck, C., Mansouri, B and Eguchi, R., "Post-disaster bridge damage assessment," *Proc. Joint ISPRS and TRM Conference, Denver* (2002).
- [8] Griesser, T. and Balanis, C.A., "Backscatter analysis of dihedral corner reflectors using physical optics and physical theory of diffraction," *IEEE Transactions on Antennas Propagation* 25, 1137-1147 (1987).
- [9] Lee, J.S., Ainsworth, T.L., Krogagor, E. and Boerner, W.-M., "Polarimetric Analysis of Radar Signature of a Man-made Structure," *Proc. 2006 IEEE International Geoscience and Remote Sensing Symposium and 27th Canadian Symposium on Remote Sensing (IGARSS 2006), Denver, Colorado* (2006).
- [10] Soergel, U., Cadario, E., Thiele, A. and Thoennessen, U., "Feature Extraction and Visualization of Bridges Over Water From High-Resolution InSAR Data and One Orthophoto," *IEEE Journal of Selected Topics in Applied Earth Observations and Remote Sensing* 1, 147-153 (2008).
- [11] Raney, R.K., "Radar Fundamentals: Technical Perspective," Henderson, F.M. and Anthony, J. L. (Eds.): *Manual of Remote Sensing 3rd Edition: Principles and Applications of Imaging Radar*, vol. 2, pp. 9-130 (1998).
- [12] Robalo J. and Lichtenegger J., "ERS-SAR Images a bridge," ESA, *Earth Observation Quarterly* [Online], available at: <http://esapub.esrin.esa.it/eoq/eoq64/bridge.pdf>, pp. 7-10 (Dec. 1999).
- [13] Kerr, R.A. and Stone, R., "A Human Trigger for the Great Quake of Sichuan?" *Science* 323, 322 (2009).
- [14] Wang, Z., "A preliminary report on the great Wenchuan earthquake", *Earthquake Engineering and Engineering Vibration* 7, 225-234 (2008).
- [15] Perissin, D. and Ferretti, A., "Urban target recognition by means of repeated spaceborne SAR images," *IEEE Transactions on Geoscience and Remote Sensing* 45, 4043-4058 (2007).
- [16] Perissin, D., Prati, C., Rocca, F., Li, D.R. and Liao, M.S., "Multi-track PS analysis in Shanghai," *Proc. ENVISAT 2007, Montreux, Switzerland* (2007).
- [17] Perissin, D., Rocca, F. and Wang, T., "DEM retrieval and landslide monitoring in Badong, Three Gorges, China by means of InSAR partially coherent targets," *Proc. Dragon Symposium 2007, Aix en Provence, France* (2007).
- [18] Ferretti, A., Prati, C. and Rocca, F., "Permanent scatterers in SAR interferometry," *IEEE Transactions on Geoscience and Remote Sensing* 39, 8-20 (2001).
- [19] Brenner, A. and Roessing, L., "Radar Imaging of Urban Areas by Means of Very High-Resolution SAR and Interferometric SAR", *IEEE Transactions on Geoscience and Remote Sensing* 46, 2971-2982 (2008).
- [20] Soergel, U., Thoennessen, U., Brenner, A. and Stilla, U., "High-resolution SAR data: new opportunities and challenges for the analysis of urban areas", *IEE Proceedings Radar, Sonar & Navigation* 153, 294-300 (2006).